Cellulose (2014) 21:3487–3496
DOI 10.1007/s10570-014-0364-6

ORIGINAL PAPER

Modification of cellulose nanocrystal-reinforced composite hydrogels: effects of co-crosslinked and drying treatment

Jun Yang · Jing-Jing Zhao · Xue-Ming Zhang

Received: 12 December 2013 / Accepted: 12 July 2014 / Published online: 24 July 2014

Abstract The synthesis platform of composite hydrogels containing rigid reinforcing filler cellulose nanocrystals (CNCs) and polymer matrix polyacrylamide (PAM) has been proposed (Yang et al. in Cellulose 20:227–237, 2013). The features of CNCs as multifunctional crosslinkers and flexible polymer chain entanglements contributed to the unique arrangement of CNC/PAM clusters with reversible network structures. In this article, the chemical crosslinking agent *N,N′*-methylene-bisacrylamide (BIS) was added to obtain the dual crosslinked networks, and the mechanical properties of the resulting co-crosslinked hydrogels were examined by tailoring the CNC and BIS concentrations. The results indicated that the homogeneous dispersion of CNCs throughout the polymer matrix was disturbed in the presence of BIS, and the covalent crosslinkers led to weakness and brittleness of the hydrogels. Some new entanglements within the networks were formed after a simple drying treatment, which was verified by the greater tensile strength compared with the as-prepared ones. The mechanism for the formation of these new entanglements was ascribed to the irreversible rearrangement of the CNC/PAM network structure, whereas for co-crosslinked hydrogels no strength increment was observed after the drying treatment.

Keywords Nanocomposites · Hydrogels · Cellulose · Co-crosslink · Drying treatment

Introduction

Hydrogels are defined as three-dimensional polymer networks swollen by large amounts of trapped water or biological fluids while remaining insoluble (Appel et al. 2012; Vermonden et al. 2012; Yu et al. 2013). For a long time, enhancing the mechanical properties of hydrogels has been a critical issue in the field of gel science because of the poor mechanical behaviors of most synthetic hydrogels (Henderson et al. 2010; Wu et al. 2011; Zhao 2014). Some tough and flexible hydrogels with unique network structures, such as the nanocomposite hydrogels (NC gels) proposed by Haraguchi (Haraguchi and Takehisa 2002) and double-network gels pioneered by Gong (Gong et al. 2003), are the two typical models for preparation of hydrogels with enhanced mechanical properties.

Cellulose is the most abundant natural compound on earth, acting as a versatile building block for

---

Electronic supplementary material The online version of this article (doi:10.1007/s10570-014-0364-6) contains supplementary material, which is available to authorized users.

J. Yang (✉) · X.-M. Zhang
MOE Key Laboratory of Wooden Material Science and Application, Beijing Forestry University, Beijing, China
e-mail: yangjun11@bjfu.edu.cn

J.-J. Zhao
Beijing SL Pharmaceutical Co., Ltd., Beijing, China

biological materials (Klemm et al. 2011; Moon et al. 2011; Siró and Plackett 2010). Currently, the application of rod-like cellulose nanocrystals (CNCs), with diameters ranging from 5 to 20 nm and lengths exceeding several micrometers, is attracting increasing interest, and these natural fiber-derived composites are envisioned as an emerging new class of benign materials (Favier et al. 1995; Larsson et al. 2010; Miao and Hamad 2013). CNCs can be viewed as functional and robust fillers for multitude applications because of the benefits of renewability, biodegradability, low density, and high tensile strength (Trovatti et al. 2013; Way et al. 2012). Therefore, CNCs have been blended with a wide range of soft polymeric matrices to improve their stiffness and strength (Stone and Korley 2010).

Recently, a series of tough composite hydrogels consisting of rigid fillers (CNCs) and polymer matrix (polyacrylamide, PAM) with reversible and dynamic networks (Yang et al. 2013, 2014) was prepared by our group. The systematic evaluation of the effect of CNCs as multifunctional crosslinkers on mechanical properties of the composite hydrogels (herein after abbreviated as CNC gels) was performed, and the results revealed that the swelling behavior and tensile properties could be tailored over a wide range by controlling the CNCs' volume fraction, aspect ratio, surface charge density, and even surface coating. According to the scheme in Fig. 1, the network structures of CNC gels are briefly summarized as follows: (1) The PAM macroradicals in situ propagate from CNC surfaces and form the CNC/PAM clusters with a unique core-shell structure. At the percolation threshold, corresponding to the formation of a volume-spanned network, the initial solution-like (sol) system changes to a viscoelastic (gel) behavior (Supplementary information Fig. S1). The CNC/PAM clusters interact with each other via the presence of transient interactions that dominate the viscoelastic properties of the CNC gels. (2) CNCs' surface-grafted polymer chains randomly entangle in the dynamic network, and fraction chains may trap and act with a similar effect on the modulus as actual network junctions (chemical crosslinks) would have. (3) The interfacial interactions between CNCs and the polymer matrix are labile, ranging from covalent interactions (silane coupling bridges) to noncovalent interactions (physical adsorption, hydrogen bonds), which lead to a layer of bound region near the CNC surfaces. (4) The larger aspect ratio of CNC leads to a lower percolation threshold through the continuous connectivity among neighboring CNCs. Besides, the high surface charge density (sulfate ester unit) caused by sulfuric acid hydrolysis would facilitate CNCs' homogeneous dispersion.

Taken together, it is clear that the CNC gels are distinct from the conventional chemically crosslinked gels via the small organic crosslinks (e.g., *N*,*N*′-methylene-bisacrylamide, BIS), which generally lead to random arrangements of polymer chains among neighboring crosslinks (Skelton et al. 2013). Although some preliminary work has been conducted on the properties of CNC gels, they remain elusive in comprehensive gelation processes and unraveling the role of polymer chain entanglements (Watanabe 1999). Herein, we report the synthesis of CNC gels in the presence of chemical crosslinking agents and demystify the effects of the coexistence of chemical crosslinks and physical junctions (entanglements) on mechanical behaviors. For this purpose, the hybrid network is revisited to gain a better understanding of the mechanical reinforcement, and the general architectural scheme of this series of CNC gels is shown in Fig. 2. In addition, the modifications of entanglement in the network by the drying treatment of the as-prepared gels above the glass transition temperature, T_g, were also addressed. The correlations between the microstructures and macroscopic properties were elucidated, and the polymer chain entanglement dependence of drying treatment was further clarified. Overall, the results obtained here are anticipated to have more far-reaching implications for our ability to tailor the properties of the cellulose composites.

Experimental section

Materials

The acrylamide (AM), potassium persulfate (KPS), and *N*,*N*′-methylene-bisacrylamide (BIS) as monomer, initiator, and organic crosslinker, respectively, were all the same as in the previous work (Yang et al. 2013). The CNCs isolated from pulp (polar wood) via sulfuric acid hydrolysis were prepared and modified by organosilane γ–methacryloxypropyl trimethoxy silane (Sigma) to anchor the silane bridges (Yang et al. 2013).

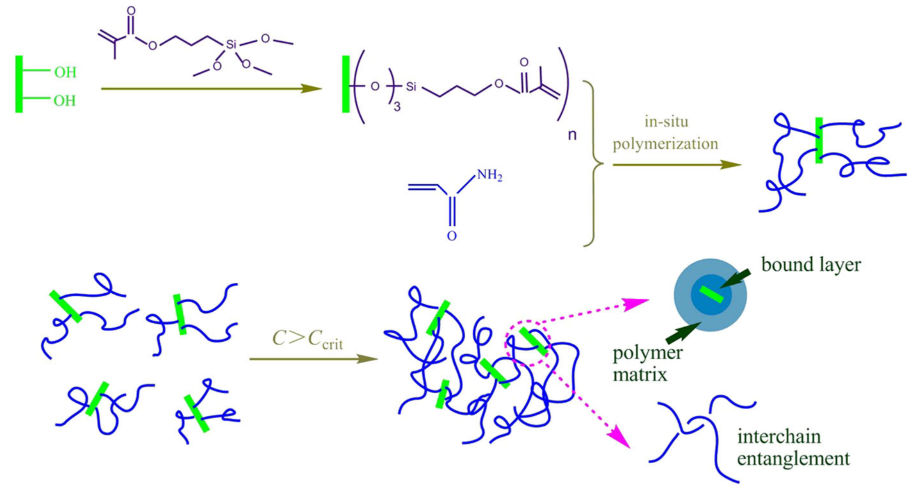

Fig. 1 Schematic preparation and structure of CNC/PAM nanocomposites. The polymer chains (*blue curves*) in situ graft from silane-modified CNC (*green bars*) surfaces to form a core-shell structure. The region near the interfacial region is restricted in its mobility, behaving like a glassy state at an attractive planar surface. With increasing distance from the CNC surface, the polymer chains have a comparable mobility to the matrix region, where two chains cannot pass through one another and create topological interactions known as entanglements, thereby contributing to the viscoelastic properties of the materials

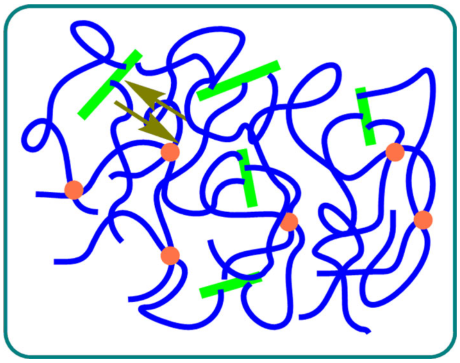

Fig. 2 Schematic presentation of co-crosslinked CNC-PAM gels combining covalent crosslinks (*orange dots*) and physical interactions (*arrows*)

Synthesis of CNC-PAM hydrogels

The sample codes for physical hydrogels, and co-crosslinked hydrogels were named CNC*x* and CNC*x*-CC*y*, respectively, according to the amount of CNC (*x* wt% against H_2O) and BIS (*y* wt% against AM). The weight of water and AM was given by 30 and 3 g, respectively, for all the procedures (Table S1). The synthetic procedure described herein was almost the same as the previously outlined procedures (Yang et al. 2013). For example, to prepare CNC0.2 gels, a mixture of water (30 g), CNC (60 mg), and AM (3 g) was prepared. The suspension was then ultrasonically dispersed (100 W) in an ice-water bath for 20 min to homogenize and break down the CNC aggregates. After degassing, an aqueous solution of initiator (KPS, 20 mg in 1 ml H_2O) was added to the above suspension under stirring, and the free radical polymerization was allowed to proceed at 45 °C under N_2 atmosphere for 90 min. For the CNC-CC gels, they were prepared with the same procedure by using CNC + BIS as crosslinks. All the as-prepared hydrogels were purified by immersion in excessive water for 72 h at 25 °C to remove water-soluble fractions. To quantitatively measure samples with different CNC and BIS fractions, the mechanical behaviors were examined at the gel preparation conditions. According to differential scanning calorimetry measurement, the glass transition temperature (T_g) of PAM is 165 °C.

Drying treatment

Here we use the term “drying treatment” to distinguish from the “as-prepared” hydrogels, that is, the above dried gels were allowed to heat further at vacuum conditions (Fig. 3). The specific procedures were performed as follows: an “as-prepared” CNC gel (swollen ratio ∼ 10) was dried in mild conditions in an air-circulation oven at 70 °C for 48 h (water content < 5 wt%). Then, the above-dried gels were

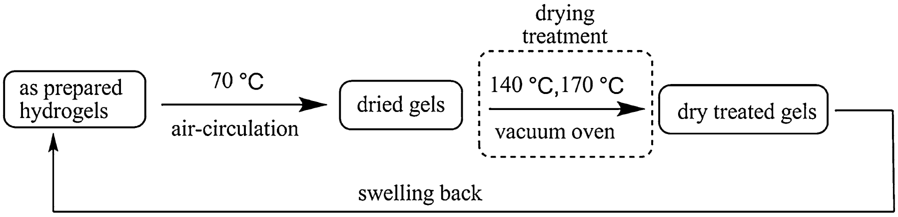

Fig. 3 Schematic illustration of drying treatment on hydrogels

allowed to undergo further drying treatment at a higher temperature [140 or 170 °C, far below the cellulose degradation temperature of about 220 °C (Klemm et al. 2011)] in a vacuum oven for 24 h. Finally, the treated gels were immersed in water and swollen back to their "as-prepared" state at 25 °C, then sealed tightly to avoid water evaporation until tensile measurements.

Characterization

Viscosity measurements

Oscillatory shear rheology measurement was conducted by a Physica MCR301 (Antor Paar Rheometer), operating with cone geometry (26.67 mm in diameter, 40.02 mm in length) under N_2 atmosphere at 45 °C. The values of the storage modulus (G') and loss modulus (G'') were recorded over the frequency range of 0.01–100 Hz at a strain of 0.01, which was within the linear viscoelastic region, as determined by dynamic strain sweep experiments. The free radical polymerization solution was transferred into liquid nitrogen at different times, t, and the reaction was quenched. The sample was recovered by subsequent dialysis against water for 2 days, dried in the vacuum oven at 60 °C for 48 h, and weighed. The time-dependent monomer conversion ratio was defined by $W(t)/W_o$, where $W(t)$ was the weight of the recovered gel at quench time t and W_o was the weight of initial monomer weight.

Transmission electron microscopy

The synthesized CNC gels were imaged on a JEM-1010 (JEOL) transmission electron microscope (TEM) at an acceleration voltage of 80 kV. The thin samples were prepared using a microtome, ultrasonicated for 10 min, and collected on copper grids (stained with 2 wt% uranyl acetate aqueous solution ~ 20 s) for morphological observation.

Mechanical properties

The uniaxial tensile stress-strain properties were examined using a Zwick Z005 Materials Tester with a load cell of 500 N at 25 °C, imposing a crosshead speed of 30 mm/min. Raw data were recorded as force versus displacement, and they were converted to stress versus strain with respect to the initial sample dimensions (5×8 mm^2). Young's modulus was calculated from the increase in load detected from elongations of 5–15 %. For each group in the test, three parallel samples were applied to ensure no obvious difference (±5 %) was observed in the stress-strain curves.

Results and discussion

Viscosity measurement

During the initial solution preparation stage, the viscosity of the aqueous suspension depended on the CNC concentration (Fig. 4a), and it showed no well-defined characteristic rheological changes as a function of time for a given CNC concentration. This result suggests that there was no interaction between fillers (CNCs) and monomers (AM) before the polymerization onset, but during the free radical polymerization stage, there was a sharp increase in viscosity for both CNC gels and CNC-CC gels (Fig. 4b). In the case of CNC0.2 gel, it exhibited a viscous gel-like material after ~50 min, and this phenomenon was related to the initially isolated CNC-PAM clusters transferring to the hydrodynamic screening region. However, in the case of CNC0.2–CC0.7 gel, it was interesting to find that the viscosity increased more rapidly than that of the CNC0.2 gel, and this increase in viscosity was steeper in the initial 45 min. However, for the CNC gels prepared in the presence of 0.2 wt% native CNC (without silanization

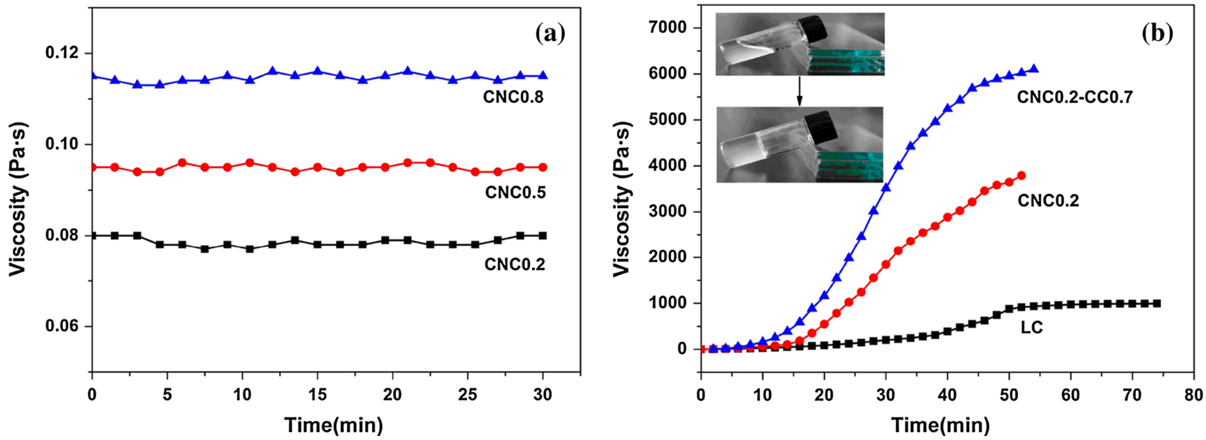

Fig. 4 Viscosity of systems as a function of time **a** before and **b** during polymerization. The images inserted in (**b**) showed transformation from free-moving liquid to a free-standing gel

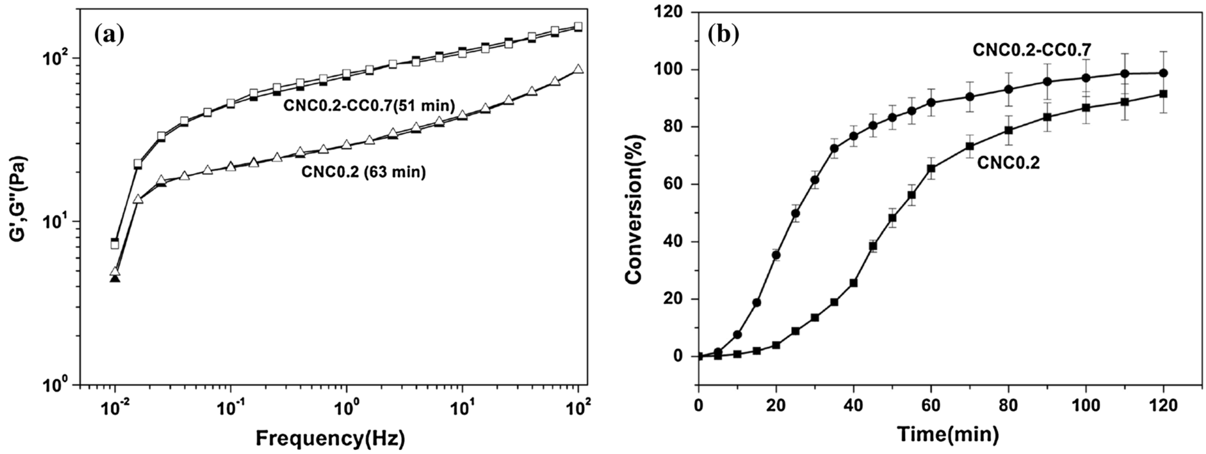

Fig. 5 **a** Elastic modulus, G′ (*open symbols*), and viscous modulus, G″ (*full symbols*), as a function of the frequency and **b** monomer conversion ratio for CNC0.2 gels and CNC0.2–CC0.7 gels

treatment), the systems could only form free linear chains (LC), and there were no covalent interactions between CNC and PAM. Thus, the viscosity of the LC solution increased slowly at the initial stage until it attained a low plateau after about 1 h. In fact, this increase in viscosity for the LC solution was ascribed to the temporary entanglements between linear polymer chains with a finite lifetime, which may break or reform continuously (Heymans 2000).

Since liquid- and gel-like behaviors of elastomers are distinguished from the frequency dependence of the storage modulus (G') and loss modulus (G'') (Martin and Adolf 1991; Rubinstein and Colby 2003), we determined the gel point by the rule that the values of G' and G'' follow the same frequency dependence ($G' \approx G'' \approx \omega^n$). The results indicated that the gel point for the co-crosslinked network (CNC0.2–CC0.7) appeared much earlier than that of the CNC0.2 gel (Fig. 5a). In addition, the monomer conversion curves as a function of time are shown in Fig. 5b, where the gel transition rate of co-crosslinked gels is also much higher than that of CNC gels. Thus, a self-consistent gelation process could be proposed in which the addition of chemical crosslinks facilitates the gelation process.

Co-crosslinked network properties

The effect of the chemical crosslinks (BIS) on the elastic and viscous properties of the co-crosslinked

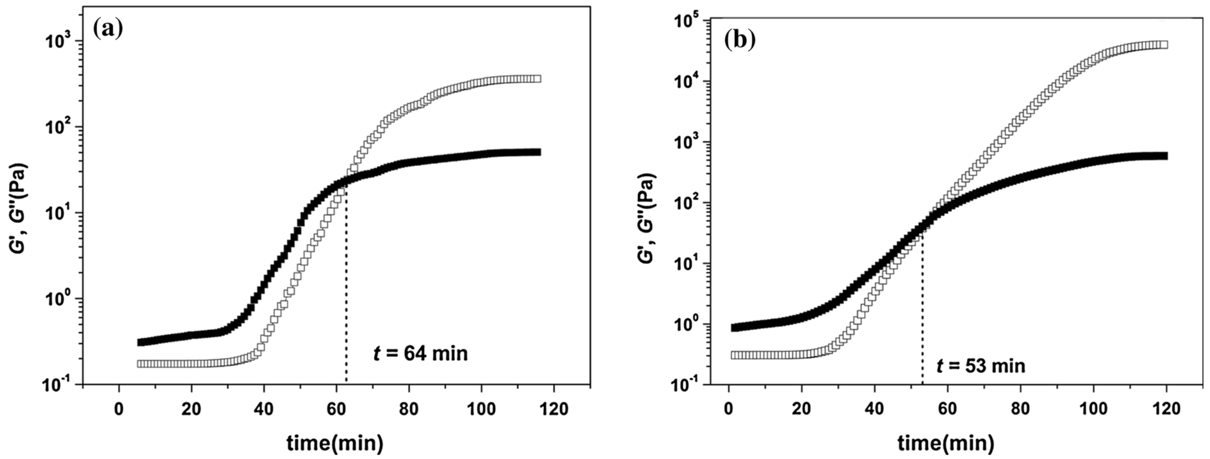

Fig. 6 Elastic moduli (*open symbols*) and the viscous moduli (*full symbols*) as a function of reaction time, *t*, for CNC0.2 (**a**) and CNC0.2–CC0.7 gels (**b**) at a frequency of 1 Hz. The defined gel time is consistent with the result in Fig. 5

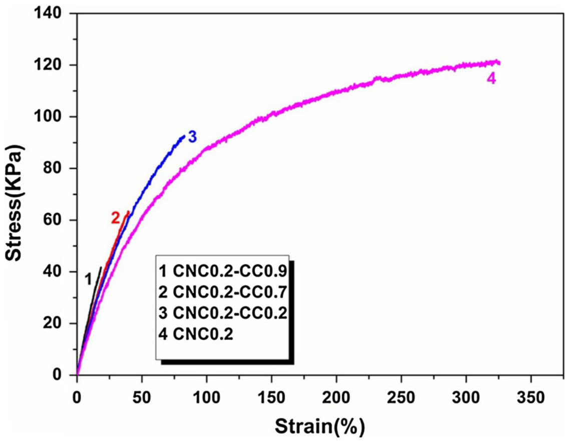

Fig. 7 Stress-strain curves for CNC0.2–CC*y* gels with different BIS contents ($y = 0.2, 0.7, 0.9$)

hydrogels is shown in Fig. 6. One can note that for CNC gels and CNC-CC gels, the general trend is a rapid increase in the modulus followed by a plateau regime in which the modulus increases slightly. The initial steep increase corresponds to the gelation process (sol-gel transition) and formation of the entangled network structure.

From the tensile stress-strain curves of the CNC-CC gels (Fig. 7), one can note that the co-crosslinked hydrogels generally showed higher Young's moduli and lower values at both the elongation ratio and strength than those of CNC gels. The brittleness of the CNC-CC gels is mainly ascribed to the limited polymer chain motions, and the role of temporary entangled junctions between CNC surface-grafted polymer chains may be restricted in this constrained system. Indeed, even using a small amount of BIS (e.g., $y = 0.2, 0.7, 0.9$) would pronouncedly jeopardize the CNC-CC gel's fracture strength and flexibility. Thus, according to their response to tensile deformation, it can be proposed that the mechanical properties of CNC-CC gels are dominated by the chemically crosslinked networks even at a very low BIS concentration.

Young's modulus of the hydrogels is basically proportional to the number of effective crosslinks, no matter whether chemically crosslinked ones or physical ones (Flory 1944; Tanaka et al. 1995). Thus, if we assume the moduli of CNC*x*–CC*y* gels are the summation of the corresponding CNC*x* and CC*y* hydrogels, the following scenario can be proposed. The actual moduli of CNC*x*–CC*y* would basically be equal to or much lower than the summary of two parts in the case of low values of x/y ($x = 0.2$, $y = 0.7$–1.4) or high values of x/y ($x = 0.2$, $y = 0.02$–0.4), respectively (Fig. 8, taking CNC0.2–CC0.7 as an example; a detailed description is given in Fig. S3). This result can be explained in that at low x/y values, CNCs are allowed to distribute homogeneously within the polymer matrix and prone to forming a percolated filler network (Fig. 9a). The physical entanglement is accessible, and the number of accompanying flexible chains that contributes to the network's moduli increases under the well-dispersed physical junctions, whereas in the case of samples at

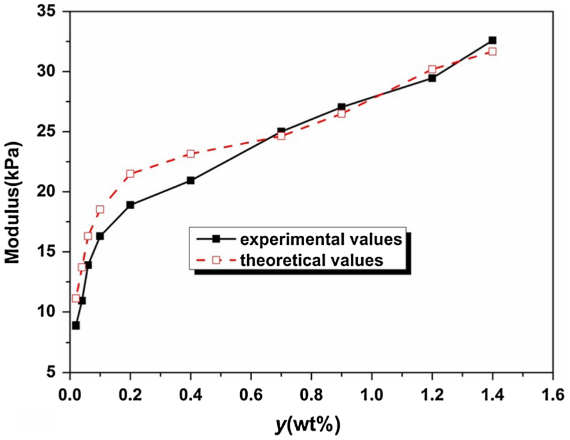

Fig. 8 Experimental and theoretical Young's modulus for CNC0.2–CC*y* gels

high *x*/*y* values, the formation of CNC clusters with a core-shell structure is disturbed in the presence the chemical crosslinks (Fig. 9b) because the BIS content at the surface of CNC may be higher than that in the PAM matrix, leading to a discontinuous CNC network and some local aggregations (indicated by arrows). In fact, even at a very low *y* (e.g., $y = 0.02$), the CNC fraction is less effective at increasing the modulus because of the presence of chemical crosslinks. That is, the entanglements formed by flexible chains are restricted, and the local topological entanglement is the lack of long distance activity. Thus, the moduli of CNC0.2–CC*y* gels are lower than the sum of CNC0.2 and CC*y* gels.

Drying treatment

Since the formation of physical entanglements by polymer chains is crucial to the viscoelastic characteristics of CNC gels, here we applied the drying treatment to tailor the degree of the entanglement level, and the corresponding structural changes were interpreted by mechanical behaviors (the effect of drying treatment on CNC was excluded by TEM observation in Fig. S4). The stress-strain curves of CNC gels after drying treatment at 140 °C are found to cause notable changes in their mechanical behaviors. As illustrated in Fig. 10, the CNC0.1 gels showed evident enhancement of the tensile mechanical properties by a simple drying treatment, such as both the greater tensile strength and modulus compared with that of the as-prepared ones (effect of the drying treatment on the swelling behavior in Fig. S5). This increase in tensile strength and modulus may be ascribed to the formation of some additional entanglements during the drying treatment, i.e., the increased frequency of polymer chain thermal motion and formation of some new entanglements near the original loose contact polymer chains. These newly produced entanglements facilitate the irreversible network conformational arrangements and therefore contribute to the greater tensile strength. However, it should be noted that if the time of drying treatment was increased (e.g. 48 or even 96 h), no further enhancement in mechanical properties could

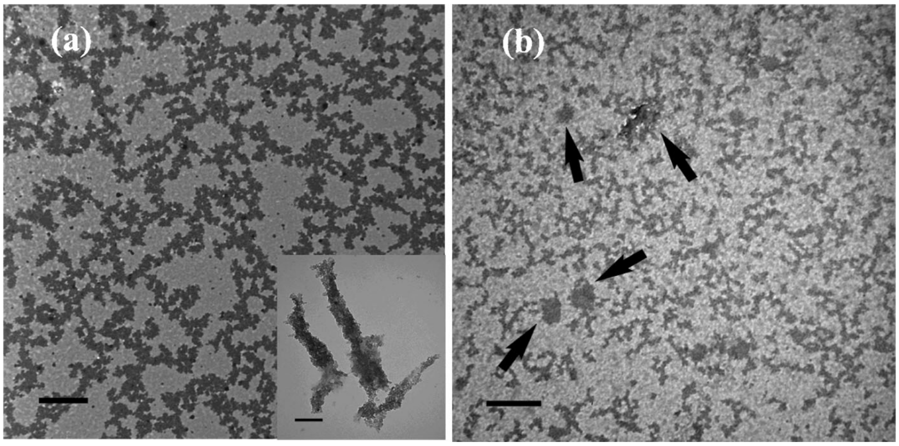

Fig. 9 TEM images of **a** CNC0.2–CC1.4 gels and **b** CNC0.2–CC0.02 gels (*bar* = 200 nm). The CNCs disperse homogeneously within the polymer matrix and form a core-shell structure (insert in (**a**), *bar* = 50 nm) where the CNCs are surrounded by polymer chains

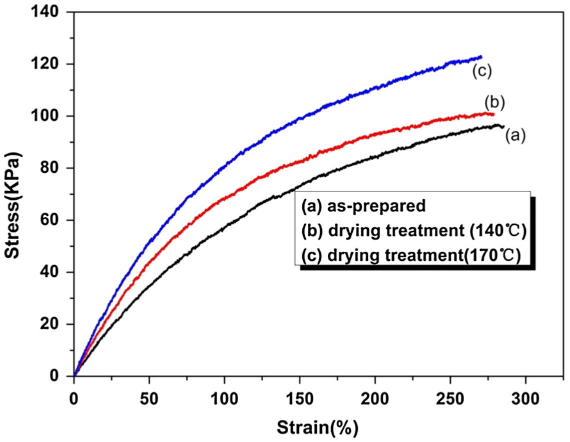

Fig. 10 Stress-strain curves of CNC0.1 gels undergo different treatment histories: (*a*) as-prepared and drying treatment at 140 °C (*b*) and 170 °C (*c*) for 24 h

be observed. Thus, the newly formed polymer chain entanglements were stable against the following drying treatment, and 24 h was adequate for CNC gels to produce topological architectural rearrangements.

Note that the effect of drying treatment on network conformational change motivates a hypothesis that the mechanical strength of CNC gels may be further enhanced if the polymer chains are allowed to rearrange to a maximal extent. With this aim in mind, the drying treatment was further conducted by drying the CNC gels slightly above the glass transition temperature ($T_g \sim 165$ °C) of the polymer matrix at 170 °C. As shown in Fig. 10, the stress-strain curves for CNC0.1 gels after drying treatment at 170 °C showed further increases in both tensile strength and Young's modulus, suggesting the degree of conformational rearrangement and inter-chain packing by micro-Brownian motions are more accessible above the T_g condition. In fact, it is widely held that the performance of polymeric materials is related to the amount of entanglement (Hintermeyer et al. 2008; Lin et al. 2012), where a higher tensile strength can be expected after polymer drying treatment at the T_g condition.

To better clarify the influence of the entanglement on mechanical properties, the hydrogels with different CNC contents were applied to drying treatment. The results indicate that the network structure at a low CNC content demonstrates a more notable enhancement in tensile strength (Fig. 11a). For example, CNC0.02 showed the highest tensile increase (38 %), followed by CNC0.04 (33 %), CNC0.08 (30 %), and CNC0.1 (26 %). This trend is reasonable if we consider that the CNCs acted as multifunctional crosslinks in the network, and the networks at a low CNC content possessed high long-range mobility among neighboring CNCs. Therefore, the gels at low CNC contents can be viewed as the mobility of segments, and inter- and intra-chain entanglements are less hindered, leading to more accessibility of the segment motions.

Furthermore, the CNC-CC gels were also applied to examine the effect of drying treatment on stress-strain properties (Fig. 11b). The results indicated that the co-crosslinked hydrogels illustrated a negligible increase in tensile strength and Young's modulus after drying treatment. For example, the CNC0.2–CC0.9 showed only a little increase in tensile strength (6.3 %) and modulus (3.5 %) after drying treatment compared with the as-prepared samples. This result suggests that the formation of additional entanglements and polymer chain rearrangement are substantially suppressed by the presence of chemical crosslinks.

Drying modification mechanism

Taking the findings together, the following mechanism for CNC gel modification after drying treatment is thereby proposed. The CNC gels formed by the free radical polymerization from CNC surfaces are stable, which was verified by the observation that there were no obvious changes in the swelling and mechanical properties under the maintained air-tight conditions (Fig. S6). However, because the entanglements among polymer chains belong to noncovalent interactions and these physical junctions are highly flexible and mobile, the application of drying treatment on the materials would facilitate CNC/PAM cluster rearrangement and closer contact. Besides, the gel networks collapse and contract in response to the evaporation of water from the original swollen state, which may lead to closer contact interactions. Since these physical entanglements act as temporary junctions, a denser entanglement is formed and presents a strengthening effect after drying treatment. Thus, when the drying treatment-modified CNC gels re-swell to their initial swollen state, these newly formed crosslinks accordingly contribute to a higher tensile strength.

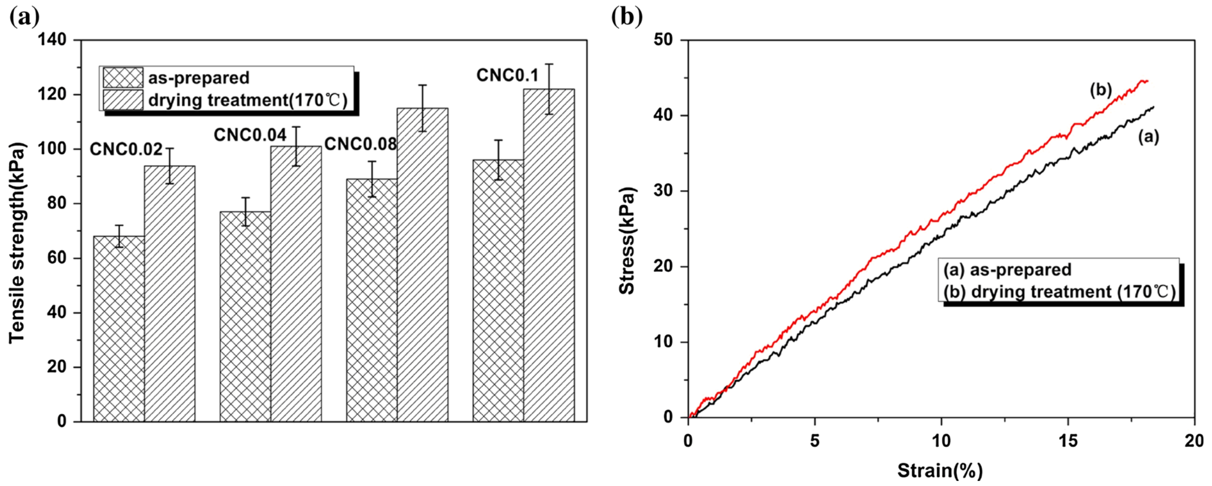

Fig. 11 Effect of drying treatment on **a** CNC*x* gels and **b** CNC0.2–CC0.9 gels

It is well known that annealing of an amorphous polymer at T_g condition is generally called sub-T_g heat treatment and affects polymer properties (Pan et al. 2007). Polymer chains demonstrate segment relaxation during the drying treatment and undergo conformational rearrangements, which lead to a dense entanglement level due to the enhanced mobility of segments. After the polymer chains have been annealed at a temperature around T_g, interpenetration and re-entanglement of the isolated polymer chains occur, and some new chain coils form via thermal diffusion. Therefore, the drying treatment can be viewed as a process in which the cohesional state of a polymeric specimen is formed and polymer chains accordingly transfer to the equilibrium state (Mi et al. 2003; Litvinov and Steeman 1999).

Conclusions

Co-crosslinked CNC/PAM hybrid hydrogels were synthesized via in situ free polymerization of AM in aqueous suspension by two types of crosslinks, a multifunctional fraction (CNC) and an organic fraction (BIS). The resulting viscosity changes during the gelation process were monitored, and the results indicated that the formation of entanglements was suppressed by the presence of BIS. The CNC*x*–CC*y* gels always showed brittle and weak properties, and the hydrogels' tensile moduli increased in proportion to the content of *x* and *y*. The tensile strength of the CNC gels after drying treatment was greater than that of the as-prepared ones, which was ascribed to the rearrangement of the single polymer coils through thermal diffusion. The additionally formed entanglements can be viewed as some temporary physical junctions that contributed to the network structure strength and increased the entanglement level, therefore leading to an increase in the tensile strength and modulus. In contrast, the co-crosslinked gels did not show any obvious increase in mechanical properties in response to drying treatment because of the chemical crosslinks' restricted polymer chain motion. The above analysis of chain entanglements by a co-crosslinked network structure and drying treatment extends the understanding of the formation of physical hydrogels from the view of irreversible conformation rearrangement and makes future fabrication of highly mechanical hydrogels, especially physically crosslinked cellulose hydrogels, more controllable and accessible.

Acknowledgments This work was financially supported by Fundamental Research Funds for the Central Universities (TD2011-10), Research Fund for the Doctoral Program of Higher Education of China (20120014120006), and Program for New Century Excellent Talents in University (NCET-12-0782).

References

Appel EA, Barrio J, Loh XJ, Scherman OA (2012) Supramolecular polymeric hydrogels. Chem Soc Rev 41:6195–6214

Favier V, Chanzy H, Cavaillé JY (1995) Polymer nanocomposites reinforced by cellulose whiskers. Macromolecules 28:6365–6367

Flory PJ (1944) Network structure and the elastic properties of vulcanized rubber. Chem Rev 35:51–75

Gong JP, Katsuyama Y, Kurokawa T, Osada Y (2003) Double-network hydrogels with extremely high mechanical strength. Adv Mater 15:1155–1158

Haraguchi K, Takehisa T (2002) Nanocomposite hydrogels: a unique organic–inorganic network structure with extraordinary mechanical, optical, and swelling/de-swelling properties. Adv Mater 14:1120–1124

Henderson KJ, Zhou TC, Otim KJ, Shull KR (2010) Ionically cross-linked triblock copolymer hydrogels with high strength. Macromolecules 43:6193–6201

Heymans N (2000) A novel look at models for polymer entanglement. Macromolecules 33:4226–4234

Hintermeyer J, Herrmann A, Kahlau R, Goiceanu C, Rössler EA (2008) Molecular weight dependence of glassy dynamics in linear polymers revisited. Macromolecules 41:9335–9344

Klemm D, Kramer F, Moritz S, Lindström T, Ankerfors M, Gray D, Dorris A (2011) Nanocelluloses: a new family of nature-based materials. Angew Chem Int Ed Engl 50:5438–5466

Larsson M, Stading M, Larsson A (2010) High performance polysodium acrylate superabsorbents utilizing microfibrillated cellulose to augment gel properties. Soft Mater 8:207–225

Lin Y, Shangguan Y, Zuo M, Jones EH, Zheng Q (2012) Effects of molecular entanglement on molecular dynamics and phase-separation kinetics of poly(methyl methacrylate)/poly(styrene-co-maleic anhydride) blends. Polymer 53: 1418–1427

Litvinov VM, Steeman PAM (1999) EPDM-carbon black interactions and the reinforcement mechanisms as studied by low-resolution ^{1}H NMR. Macromolecules 32:8476–8490

Martin JE, Adolf D (1991) The sol-gel transition in chemical gels. Annu Rev Phys Chem 42:311–339

Mi Y, Xue G, Lu X (2003) A new perspective of the glass transition of polymer single-chain nanoglobules. Macromolecules 36:7560–7566

Miao C, Hamad W (2013) Cellulose reinforced polymer composites and nanocomposites: a critical review. Cellulose 20:2221–2262

Moon RJ, Martini A, Nairn J, Simonsen J, Youngblood J (2011) Cellulose nanomaterials review: structure, properties and nanocomposites. Chem Soc Rev 40:3941–3994

Pan P, Zhu B, Inoue Y (2007) Enthalpy relaxation and embrittlement of poly(L-lactide) during physical aging. Macromolecules 40:9664–9671

Rubinstein M, Colby RH (2003) Polymer physics. Oxford University Press, Oxford

Siró I, Plackett D (2010) Microfibrillated cellulose and new nanocomposite materials: a review. Cellulose 17:459–494

Skelton S, Bostwick M, O'Connor K, Konst S, Casey S, Lee BP (2013) Biomimetic adhesive containing nanocomposite hydrogel with enhanced materials properties. Soft Matter 9:3825–3833

Stone DA, Korley LTJ (2010) Bioinspired polymeric nanocomposites. Macromolecules 43:9217–9226

Tanaka Y, Kagami Y, Matsuda A, Osada Y (1995) Thermoreversible transition of tensile modulus of hydrogel with ordered aggregates. Macromolecules 28:2574–2576

Trovatti E, Carvalho AJF, Ribeiro SJL, Gandini A (2013) Simple green approach to reinforce natural rubber with bacterial cellulose nanofibers. Biomacromolecules 14: 2667–2674

Vermonden T, Censi R, Hennink Wim E (2012) Hydrogels for protein delivery. Chem Rev 112:2853–2888

Watanabe H (1999) Viscoelasticity and dynamics of entangled polymers. Prog Polym Sci 24:1253–1403

Way AE, Hsu L, Shanmuganathan K, Weder C, Rowan SJ (2012) pH-responsive cellulose nanocrystal gels and nanocomposites. ACS Macro Lett 1:1001–1006

Wu CJ, Gaharwar AK, Chan BK, Schmidt G (2011) Mechanically tough pluronic F127/laponite nanocomposite hydrogels from covalently and physically cross-linked networks. Macromolecules 44:8215–8224

Yang J, Han CR, Duan JF, Ma MG, Zhang XM, Xu F, Sun RC (2013) Synthesis and characterization of mechanically flexible and tough cellulose nanocrystals–polyacrylamide nanocomposite hydrogels. Cellulose 20:227–237

Yang J, Zhao JJ, Han CR, Duan JF, Xu F, Sun RC (2014) Tough nanocomposite hydrogels from cellulose nanocrystals/poly(acrylamide) clusters: influence of the charge density, aspect ratio and surface coating with PEG. Cellulose 21:541–551

Yu G, Yan X, Han C, Huang F (2013) Characterization of supramolecular gels. Chem Soc Rev 42:6697–6722

Zhao XH (2014) Multi-scale multi-mechanism design of tough hydrogels: building dissipation into stretchy networks. Soft Matter 10:672–687